AMERICAN ACADEMY OF OPHTHALMOLOGY®

Histology of Type 3 Macular Neovascularization and Microvascular Anomalies in Treated Age-Related Macular Degeneration

A Case Study

Andreas Berlin, MD, MS,[1,2] Diogo Cabral, MD,[3,4] Ling Chen, MD, PhD,[1,5] Jeffrey D. Messinger, DC,[1] Chandrakumar Balaratnasingam, MD, PhD,[6,7,8] Randev Mendis, MD,[9] Daniela Ferrara, MD, PhD,[10] K. Bailey Freund, MD,[3,11] Christine A. Curcio, PhD[1]

Purpose: To investigate intraretinal neovascularization and microvascular anomalies by correlating in vivo multimodal imaging with corresponding ex vivo histology in a single patient.

Design: A case study comprising clinical imaging from a community-based practice, and histologic analysis at a university-based research laboratory (clinicopathologic correlation).

Participants: A White woman in her 90s treated with numerous intravitreal anti-VEGF injections for bilateral type 3 macular neovascularization (MNV) secondary to age-related macular degeneration (AMD).

Methods: Clinical imaging comprised serial infrared reflectance, eye-tracked spectral-domain OCT, OCT angiography, and fluorescein angiography. Eye tracking, applied to the 2 preserved donor eyes, enabled the correlation of clinical imaging signatures with high-resolution histology and transmission electron microscopy.

Main Outcome Measures: Histologic/ultrastructural descriptions and diameters of vessels seen in clinical imaging.

Results: Six vascular lesions were histologically confirmed (type 3 MNV, n = 3; deep retinal age-related microvascular anomalies [DRAMAs], n = 3). Pyramidal (n = 2) or tangled (n = 1) morphologies of type 3 MNV originated at the deep capillary plexus (DCP) and extended posteriorly to approach without penetrating persistent basal laminar deposit. They did not enter the subretinal pigment epithelium (RPE)–basal laminar space or cross the Bruch membrane. Choroidal contributions were not found. The neovascular complexes included pericytes and nonfenestrated endothelial cells, within a collagenous sheath covered by dysmorphic RPE cells. Deep retinal age-related microvascular anomaly lesions extended posteriorly from the DCP into the Henle fiber and the outer nuclear layers without evidence of atrophy, exudation, or anti-VEGF responsiveness. Two DRAMAs lacked collagenous sheaths. External and internal diameters of type 3 MNV and DRAMA vessels were larger than comparison vessels in the index eyes and in aged normal and intermediate AMD eyes.

Conclusions: Type 3 MNV vessels reflect specializations of source capillaries and persist during anti-VEGF therapy. The collagenous sheath of type 3 MNV lesions may provide structural stabilization. If so, vascular characteristics may be useful in disease monitoring in addition to fluid and flow signal detection. Further investigation with longitudinal imaging before exudation onset will help determine if DRAMAs are part of the type 3 MNV progression sequence.

Financial Disclosure(s): Proprietary or commercial disclosure may be found after the references.

Supplemental material available at www.ophthalmologyscience.org.

Type 3 macular neovascularization (MNV) is a subtype of neovascular age-related macular degeneration (AMD).[1] Unlike type 1 MNV, which arises from the choroid, type 3 MNV originates in the neurosensory retina.[2,3] Female gender, older age, and presence of subretinal drusenoid deposits confer risk of type 3 MNV.[4,5] Type 3 MNV is diagnosed in a third of White patients presenting with unilateral neovascular AMD[6] and may be underestimated overall. Fellow eyes often convert to neovascular AMD within 3 years.[7–9] Early lesions respond well to

https://doi.org/10.1016/j.xops.2023.100280
ISSN 2666-9145/23

intravitreal anti-VEGF therapy, unlike chronic lesions.[2,10] New information about type 3 MNV and related vascular anomalies from histopathology, as provided here, could support improved detection and treatment decisions in affected patients.

Recent clinical imaging studies have elucidated type 3 MNV pathophysiology. Three stages are defined based on structural OCT. Precursors to stage 1 are hyperreflective foci (HRF) at the level of the deep capillary plexus (DCP), often near drusen. Stage 1 includes an intraretinal hyperreflective lesion and cystoid macular edema. In stage 2, outer retinal disruption appears. At stage 3, the hyperreflective lesion extends into the sub-retinal pigment epithelium (RPE)–basal lamina (BL) space, associated with a pigment epithelium detachment.[2] By color fundus photography, fluorescein angiography (FA), and OCT, type 3 MNV exhibits a specific regional distribution and pattern of hemorrhage.[11–13] Lesions localize preferentially to the inner ring of the ETDRS grid. Flame-shaped intraretinal hemorrhages are located over type 3 MNV lesions, pointing toward the fovea. OCT angiography (OCTA) with 3-dimensional reconstruction and display shows vertically oriented components of type 3 MNV. Using this technology, Borrelli et al[14] describe 2 morphologic phenotypes ("filiform" and "saccular") of advanced type 3 MNV.

Prior clinicopathologic correlation has elucidated some cellular detail corresponding to the OCT-based stages.[15,16] Neovascular complexes originating at the DCP have a vertical and downward trajectory. These complexes expand posteriorly and cross a persistent basal laminar deposit (BLamD) to enter the sub–RPE-BL space. Some complexes seem like base-down pyramids that are ensheathed by collagenous material.[3,16] Participatory cells include macrophages, VEGF-positive fibroblasts, lymphocytes, Müller cell processes, and subducted RPE cells.[15,16] Hence, ischemia and inflammation may promote the development and progression of type 3 MNV.[15,16]

Microvascular abnormalities involving the DCP include microaneurysms, telangiectasia, perifoveal exudative anomalous vascular complex, and capillary macroaneurysms.[17–22] Perifoveal exudative anomalous vascular complex was initially described in non-AMD eyes as an isolated aneurysmal dilation of a retinal capillary originating between the superficial and deep plexuses, with exudation that is unresponsive to anti-VEGF.[17,22,23] Deep retinal age-related microvascular anomalies (DRAMAs) are recently proposed as DCP alterations in the setting of AMD findings, such as soft drusen and intraretinal HRF. Eyes with DRAMA show abnormal horizontal or vertical vessels with a diameter of > 50 μm and/or a location below the posterior border of the outer plexiform layer (OPL).[24] In contrast to type 1 MNV,[25] precursors, early stages, and potential masqueraders for type 3 MNV, which may include DRAMA, are not described at the histologic level.[26] Human eyes with longitudinal clinical imaging are especially valuable sources for such information.[3]

Here, we directly compared longitudinal OCT and angiographic signatures of intraretinal neovascularization and microvascular anomalies with the corresponding histology. We analyzed both eyes of a single patient who had received intravitreal anti-VEGF treatments for type 3 MNV over the course of 5 years (right eye [OD]) and 9 months (left eye [OS]).

Methods

Compliance

Approval for this study was obtained by an institutional review board at the University of Alabama at Birmingham (protocol #300004907). The study was conducted in accordance with the tenets of the Declaration of Helsinki and the Health Insurance Portability and Accountability Act of 1996.[27,28]

Clinical Course

A White, pseudophakic woman in her 90s received comprehensive ophthalmic examination and multimodal imaging during a 5-year follow-up for bilateral type 3 MNV secondary to AMD. The patient presented 5 years before death with exudative type 3 MNV in the OD. Over 5 years, she received a total of 37 intravitreal anti-VEGF injections over ~6 fluid resorption cycles in the OD (12 × 0.5 mg/0.05 ml ranibizumab, then 25 × 2 mg/0.05 ml aflibercept). One fluid resorption cycle is defined as the time in weeks and the number of injections needed from initial detection of intraretinal/subretinal edema on OCT until complete absence of edema on OCT. The OS was diagnosed with exudative type 3 MNV 4 years after the OD. Over 9 months, the OS received a total of 6 intravitreal anti-VEGF injections over ~2 fluid resorption cycles (12 × 0.5 mg/0.05 ml ranibizumab). Her general medical history included dyslipidemia and paroxysmal atrial fibrillation. Six months before death, the patient was diagnosed with gallbladder adenocarcinoma. Her last anti-VEGF treatment before death due to adenocarcinoma was 3 and 2 months for the OS and OD, respectively.

Clinical Image Capture and Analysis

All images were acquired using Spectralis HRA + OCT (Heidelberg Engineering). Available for review were 11 (OD) and 7 (OS) eye-tracked spectral-domain OCT volumes (6 × 6 mm horizontal and radial scans; 20° × 20° field). Fluorescein angiography was available for both eyes at first presentation and 4 years later.

One eye-tracked spectral-domain OCTA volume (3 × 3 mm horizontal scans, 256 B-scans at 6-μm spacing, 10° × 10° field, automatic real-time tracking [ART 5], quality 34 dB) was obtained of the OD 3.5 years after presentation.[29] An investigational version of Heidelberg Eye Explorer (version 6.16.100.701, Heidelberg Engineering) was used for analysis, processing, and postprocessing of data.[3,30] Projection artifact was removed via 3-dimensional vessel-shape estimation and a Gaussian blur filter.[3,30] Raw (floating point) data were exported as a.VOL file.

Volume rendering enhances visualization of type 3 MNV, which is vertically oriented, and allows afferent/efferent vascular connections to be identified, particularly in deeper retinal layers.[3,31] To visualize lesions at different angles of rotation, OCTA B-scans were first processed using linear quadratic estimation (noise variance estimate of 0.05 and a gain of 0.8; MATLAB version R2019b, The MathWorks Inc; 2019), followed by volume rendering and analysis (Imaris version 9.5, Bitplane, Andor Technology plc).[32] The Filament Tracer tool was used to trace superficial arteries and veins after evaluation of dye circulation in FA. Video recording and still images were annotated to highlight structural and flow details.

Previous reports indicated both eccentricity- and hemifield-dependent asymmetries in the spatial distribution of type 3

MNV.[11,12,33] Thus, for potential mechanistic insight into tissue-level associations, location of vascular lesions was documented. Lesion distance from the fovea was calculated using the OCT volume and near-infrared reflectance imaging en face image using a custom ImageJ plug-in "Spectralis Browser OCT," available at https://sites.imagej.net/CreativeComputation/. Meridional position was documented using the sectors of the ETDRS grid.[34,35]

Histology Preparation and Image Analysis

As described,[36] globes were recovered 2 hours 5 minutes after death and preserved in buffered 1% paraformaldehyde and 2.5% glutaraldehyde. Premortem eye-tracked OCT volumes were registered to postmortem OCT volumes of the same globes.[37] For high-resolution histology over large areas, a rectangular tissue block containing the fovea and optic nerve was postfixed in 1% osmium—tannic acid—paraphenylenediamine and embedded in epoxy resin. A tissue block 8 × 12-mm wide was processed for stepped sections at 30- to 60-μm intervals. Interleaved 30-μm thick slabs were reembedded for transmission electron microscopy. Submicrometer sections stained with toluidine blue were scanned using a 60X oil immersion objective.[38] Tissue sections on 112 (OD) and 87 (OS) glass slides spanning a distance of 5453 μm (OD) and 4243 μm (OS) centered on the 2 foveas were matched to clinical OCT scans by comparing overall tissue contours.

Deep retinal age-related microvascular anomaly vessels are defined by a diameter criterion (> 50 μm),[24] and our previous and current observations indicated that a collagenous sheath surrounds type 3 MNV neovessels. Furthermore, OCTA shows only the moving blood cell column and not the collagenous sheath. Therefore, we manually measured internal (luminal) and external cross-sectional diameters of vessels ("oval" tool, FIJI Is Just; ImageJ 2.0.0-rc- 69/1.52p; www.fiji.sc). Type 3 MNV vessels meandered over several glass slides, and sections on each slide were measured. To contextualize neovessel measurements, DCP vessels on either side of the area directly involved in exudation in the index case were also measured. Furthermore, vessels aligned along the outer border of the inner nuclear layer (INL) of intermediate AMD eyes and age-similar controls (n = 8 each) on the Project MACULA website of AMD histopathology were also measured.[25] Because vessels could run longitudinally within a section, we report a minimal cross section diameter (approximated by Feret diameter in ImageJ for ellipses). Because of small numbers, these data were not analyzed statistically.

Results

Table S1 (available at www.ophthalmologyscience.org) lists all figures to provide an overview.

Classification of Lesions and Longitudinal Clinical Imaging

We first classify vascular complexes in the 2 eyes at one time point and then describe them in longitudinal clinical imaging and detailed histology. Table 2 lists hyperfluorescent lesions seen by FA 11 months before death (Fig 1). Six of 7 lesions localized to the inner ring of the ETDRS grid (0.5−1.5 mm eccentricity), with the seventh at 1.52 mm. There was no predilection for any 1 sector. Six of 7 lesions were confirmed as vascular by histology, and the seventh (Fig S2, available at www.ophthalmologyscience.org) could not be found. Lesion morphology was categorized as tangled type 3 MNV (n = 1), pyramidal type 3 MNV (n = 2), or DRAMA (n = 3). As seen previously,[3,16] pyramidal type 3 MNV was defined as a focal, vertically extending neovessel complex. Tangled type 3 MNV was defined as a horizontally extending neovessel complex. Deep retinal age-related microvascular anomaly was defined as anomalous vascular elements extending posterior to the DCP and into the Henle fiber layer (HFL)/outer nuclear layer (ONL), that is, anterior to the external limiting membrane (ELM).[24] Hyperfluorescent lesions in the OD due to window defects were reported elsewhere.[39]

At initial presentation 5 years before death, the OD exhibited multiple instances of MNV secondary to AMD with multifocal leakage on FA (Fig S3, available at www.ophthalmologyscience.org). At this time, fluid was not detected in the OS (Fig S4, available at www.ophthalmologyscience.org). Four years later and 11 months before death (Fig 1), the OS was diagnosed with exudative type 3 MNV because of AMD. By this time, the OD had received 32 intravitreal anti-VEGF injections at intervals of 4 to 8 weeks resulting in 4 fluid resorption cycles.

Pyramidal (OD 2, OS 4) and Tangled (OD 1) Type 3 MNV

Pyramidal type 3 MNV (OS 4) closely resembles previously described OD 2[4] in terms of location, OCT appearance, and histologic features (Figs 1, 5, 6, respectively). In brief, OS 4 is a vertically oriented, pyramidal-shaped, intraretinal lesion located in the nasal sector of the ETDRS inner ring, with heterogeneous hyperreflectivity on OCT (Fig 5). On histology, this lesion corresponds to a collagen-ensheathed neovascular complex that extends from the OPL/INL border through the HFL/ONL (Fig 6A). The complex is flanked by RPE cells that extend off the top of the pyramid and along a DCP vessel (Fig 6B). The pyramid base adheres to denuded and persistent BLamD, which drapes a calcified druse (Fig 6A, B).[4] The vessel did not enter the sub−RPE-BL space, and no choroidal contribution was found.

Transmission electron microscopy of this pyramidal lesion reveals endothelial cells and pericytes (Fig 7A). Endothelial cells are not fenestrated (Fig 7B), like endothelial cells of the DCP and unlike endothelial cells of the choriocapillaris (Fig 7C, D). Other vessel wall components, for example, smooth muscle cells, connective tissue, or a 3-layer arterial configuration, cannot be identified. In RPE cells arrayed along the sloping sides of the calcified druse, lipofuscin becomes less electron dense, smaller, and less tightly packed (Fig 7E) in a smooth transition. These findings suggest transdifferentiation, rather than ingestion of RPE organelles by invading phagocytes.

Next, we consider tangled type 3 MNV (OD 1), for which en face OCTA (Fig 8A2) and OCT with flow overlay (Fig 8A3) shows persistent flow signal. Over time, the extent of intraretinal fluid surrounding OD 1 in the INL and HFL fluctuates (Fig 8B2, C2, respectively). Volume rendering of structural OCT and OCTA together highlights flow within a hyperreflective lesion at the ONL

Table 2. Spatial Distribution and Vascular Lesion Types in 2 Eyes of the Index Case

Eye, Lesion Number, Color in Fig. 1	ETDRS Ring and Sector	Lesion Type	Intravitreal Anti-VEGF	Analysis
OD 1 (green)*	Inner, S	T3MNV, tangled	37	LM
OD 2 (yellow)	Inner, N	T3MNV, pyramidal	37	LM
OD 3 (fuchsia)†	Inner, T	DRAMA	37	LM
OS 1 (yellow)	Inner, S	DRAMA	6	LM
OS 2 (white)	Outer, I	Not found	6	n.a.
OS 3 (fuchsia)	Inner, I	DRAMA	6	LM, EM
OS 4 (green)	Inner, N	T3MNV, pyramidal	6	LM, EM

DRAMA = deep retinal age-related microvascular anomaly; EM = electron microscopy; I = inferior; LM = light microscopy; N = nasal; n.a. = not available; OD = right eye; OS = left eye; S = superior; T = temporal; T3MNV = type 3 macular neovascularization.
ETDRS sectors (delimited by 45° lines).
Within each eye, lesions seen on fluorescein angiography were numbered clockwise, starting at 12 o'clock (ETDRS grid superior sector).
*Span width of tangled vascular lesion: 520 to 769 μm.
†Pair of vascular lesions.

and bacillary layer (Fig S9A, Video S1, available at www.ophthalmologyscience.org). Inflow and outflow vessels can be connected to a superficial artery and vein, respectively (Fig S9B, C). The RPE/Bruch membrane (BrM) complex below the lesion is split by hyporeflective material producing a double layer sign (Fig 7B2).[40] Numerous HRF are present in the INL (Fig 8C2).

Histologic analysis reveals components of tangled type 3 MNV (OD 1, Fig 8D). Magnified histology shows a vascular complex spanning 249 μm horizontally, extending into the superior perifovea (Fig S10, available at www.ophthalmologyscience.org.). The complex is partly ensheathed by collagenous material and flanked by intraretinal RPE cells. The INL/OPL border subsides where the vascular lesion extends through the HFL/ONL (Fig S10C). The ELM subsides at both edges of the calcified druse (yellow arrows in Fig S10B). Bruch membrane seems intact without evidence of a choroidal contribution to the MNV lesions or evidence of MNV contributing to the OCT double layer sign (Fig S10A–C). Neovessels within the INL are moderately dilated, suggesting drainage venules (Fig S10A).[41]

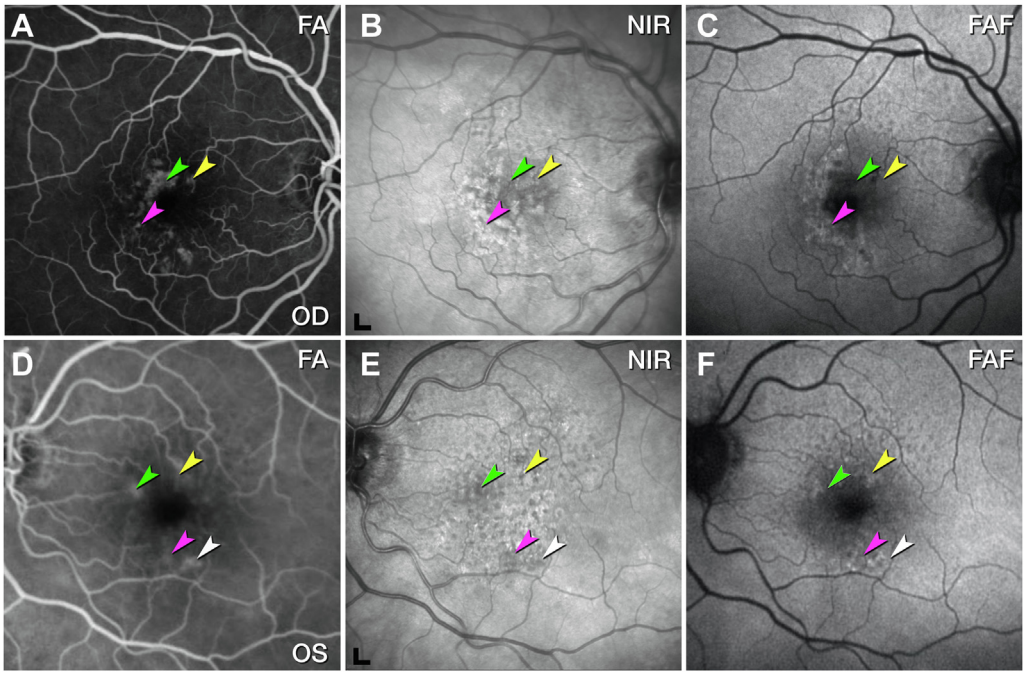

Figure 1. Multimodal retinal imaging of both eyes, 11 months before death. Fluorescein angiography (FA) in the venous (**A**) and recirculation phases (**D**) showed multiple instances of hyperfluorescence. Vessels were found by histology at the green, yellow, and fuchsia arrowheads in the right eye (**A**) and left eye (**D**). At the white arrowhead in the left eye, no vessel could be found in histology. **B**, **E**, Near-infrared reflectance imaging (NIR) shows reduced reflectance in areas of angiographic leakage (arrowheads), possibly because of retinal edema. Soft drusen exhibit hypo- and hyperreflective mottling. Scale bar = 200 μm. **C**, **F**, Fundus autofluorescence (FAF) (λ_{ex}= 488 nm) highlights subretinal drusenoid deposits, especially superior to the fovea. Lesion number, type, and spatial distribution are listed in Table 2. OD = right eye; OS = left eye.

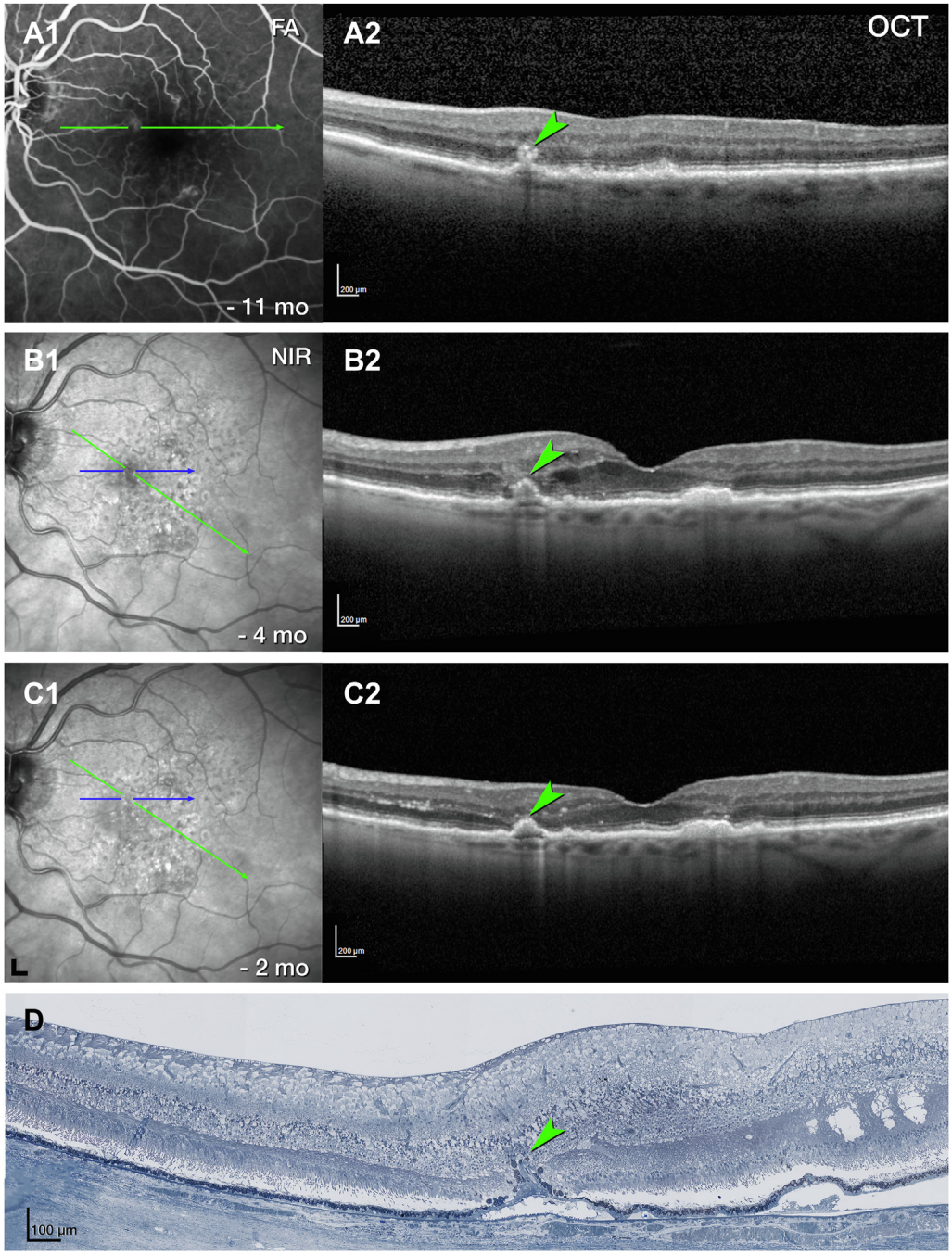

Figure 5. Multimodal imaging, clinical course, and histology of pyramidal type 3 macular neovascularization (MNV), left eye (OS) 4. **A**, Venous phase fluorescein angiography (FA) (**A1**) shows mild leakage at the site of type 3 MNV 11 months before death. Green lines on FA represent OCT B-scans. A horizontal OCT B-scan (**A2**) displays a hyperreflective lesion, hyperreflective foci (HRF), and small intraretinal cysts. **B**, Blue lines on near-infrared reflectance imaging (NIR) (**B1**) represent histology section in (**D**). Radial OCT B-scan (**B2**) displays enlarged intraretinal cysts after 5 total injections and 8 weeks after the prior injection. There is also a subsidence of the outer plexiform layer (OPL) and external limiting membrane (ELM). **C**, On radial OCT B-scan (**C2**), intraretinal fluid is reduced after 6 injections and 6 weeks after the prior injection. Numerous HRF are present in the inner nuclear layer (INL) (**C2**); scale bar = 200 µm. **D**, On histology, type 3 MNV is a pyramidal complex bounded by retinal pigment epithelium (RPE) cells. It extends from the INL/OPL border to the basal laminar deposit (BLamD) draping a calcified druse. Structural damage to the Henle fiber layer at the right of the panel (green asterisk) may indicate an area of prior intraretinal fluid. Magnified histology is shown in Figure 6. Scale bar = 100 µm. Blue line, histology section. Time in months and time before death.

To summarize, the vascular geometry and thickness of the collagenous sheath differentiate tangled versus pyramidal type 3 MNV. The sheath surrounding the tangled complex is thin (Fig S10), and that surrounding pyramidal type 3 MNV is thick (Fig 6). Otherwise, the 2 subtypes are comparable.

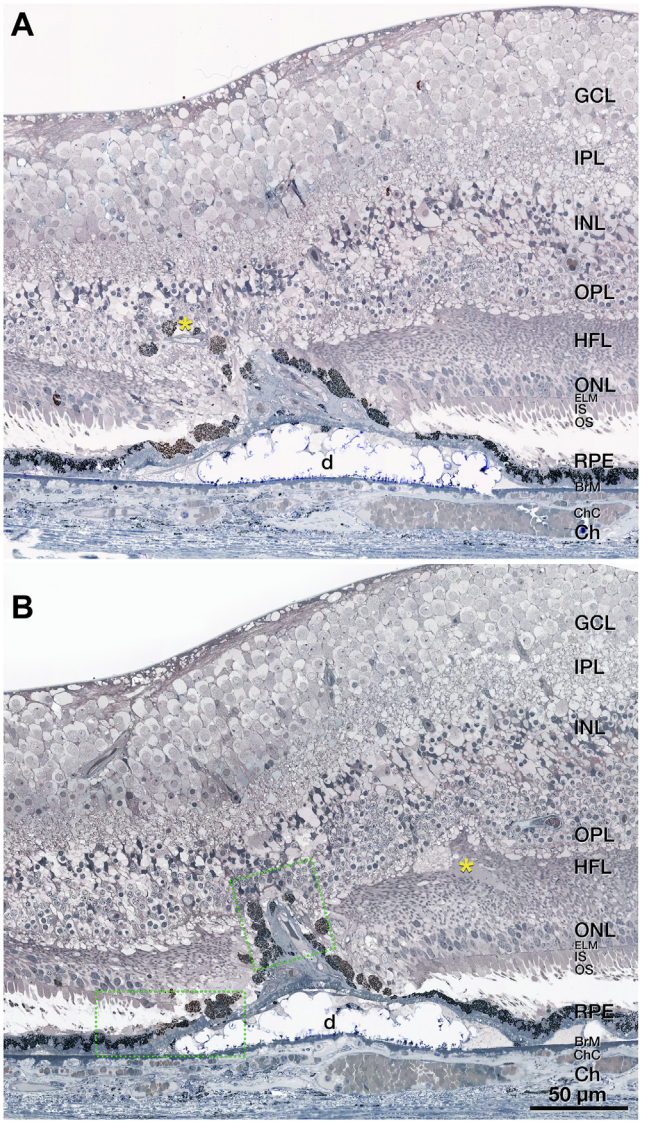

Figure 6. Pyramidal vascular complex in type 3 macular neovascularization (MNV), left eye (OS) 4. **A**, **B**, A pyramidal complex includes neovessels ensheathed by thick layers of collagenous material and flanked by retinal pigment epithelium (RPE) cells. The complex extends from the inner nuclear layer (INL) through the outer plexiform layer (OPL), Henle fiber layer (HFL), and outer nuclear layer (ONL) and terminates at the BLamDs draping a calcified druse. Bruch's membrane (BrM) seems intact with no evidence of a choroidal contribution to the neovessel complex. The external limiting membrane (ELM) descends at both sides of the type 3 MNV base. There is some fluid at the OPL–HFL border (yellow asterisk in **B**). Areas within dotted green boxes are shown in Figure S10. BLamD = basal laminar deposit Ch = choroid; ChC = choriocapillaris; GCL = ganglion cell layer; IPL = inner plexiform layer; IS = inner segment.

DRAMA in the Setting of Anti-VEGF Therapy

As shown below, all 3 instances of DRAMA (OS 1, OS 3, and OD 3) exhibit mild hyperfluorescence on venous and recirculation phase FA 11 months before death. In histology, all 3 localize above a horizontal (nondescending) ELM, signifying a lack of atrophy.

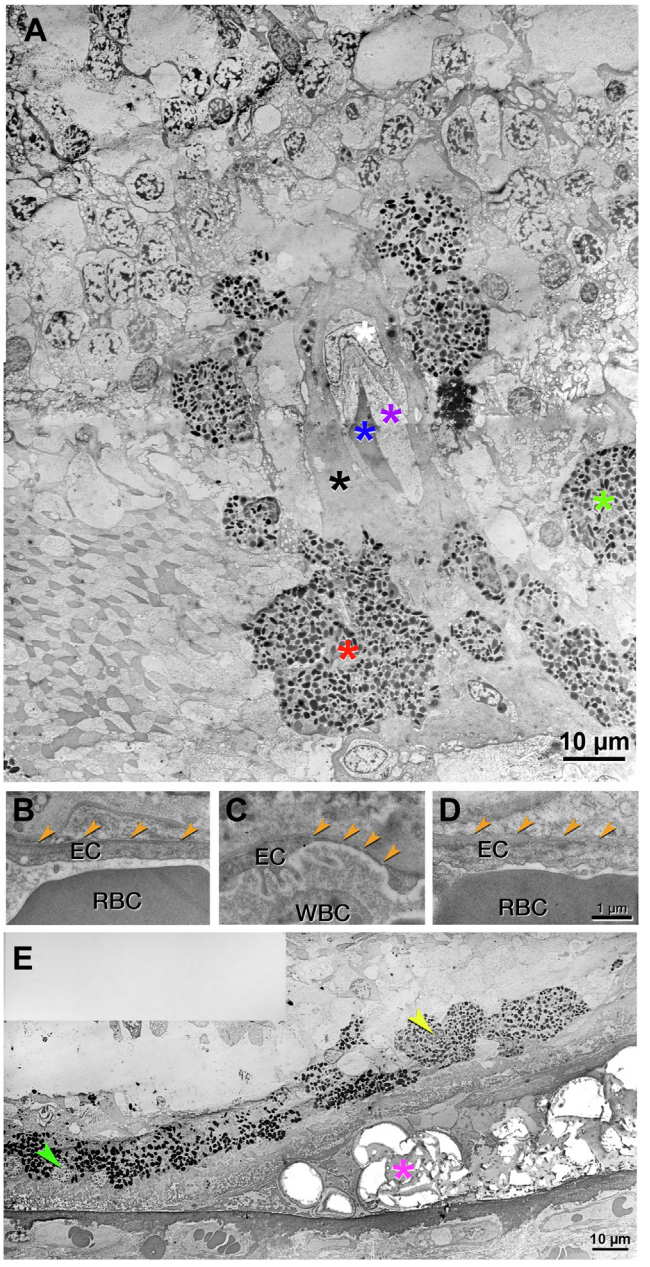

Figure 7. Transmission electron microscopy of pyramidal type 3 macular neovascularization (MNV), left eye (OS) 4. See Figure 6 for light microscopy of OS 4**. A**, Neovessel with erythrocytes in the lumen (blue asterisk) are ensheathed by endothelium, pericyte, and collagenous material (purple, white, and black asterisks, respectively). Surrounding retinal pigment epithelium (RPE) cells merge into multinucleated cells (red asterisk) or disperse into the Henle fiber layer (HFL) (green asterisk). Phagolysosomes are not visible in the RPE cells. **B**–**D**, Endothelial cells in the neovessel and comparison vessels are displayed. The lumen is located at the bottom of all the panels. **B**, No fenestrations were detected in the neovessel (orange arrowheads). **C**, Fenestrations were visible in the choriocapillaris (orange arrowheads). **D**, No fenestrations were detected in the deep capillary plexus (DCP) (orange arrowheads). **E**, Atop the calcified druse (fuchsia asterisk), RPE lipofuscin is more electron dense at the druse base than at the druse top (left versus right in the panel). These changes are consistent with transdifferentiation. EC = endothelial cell; RBC = red blood cell; WBC = white blood cell.

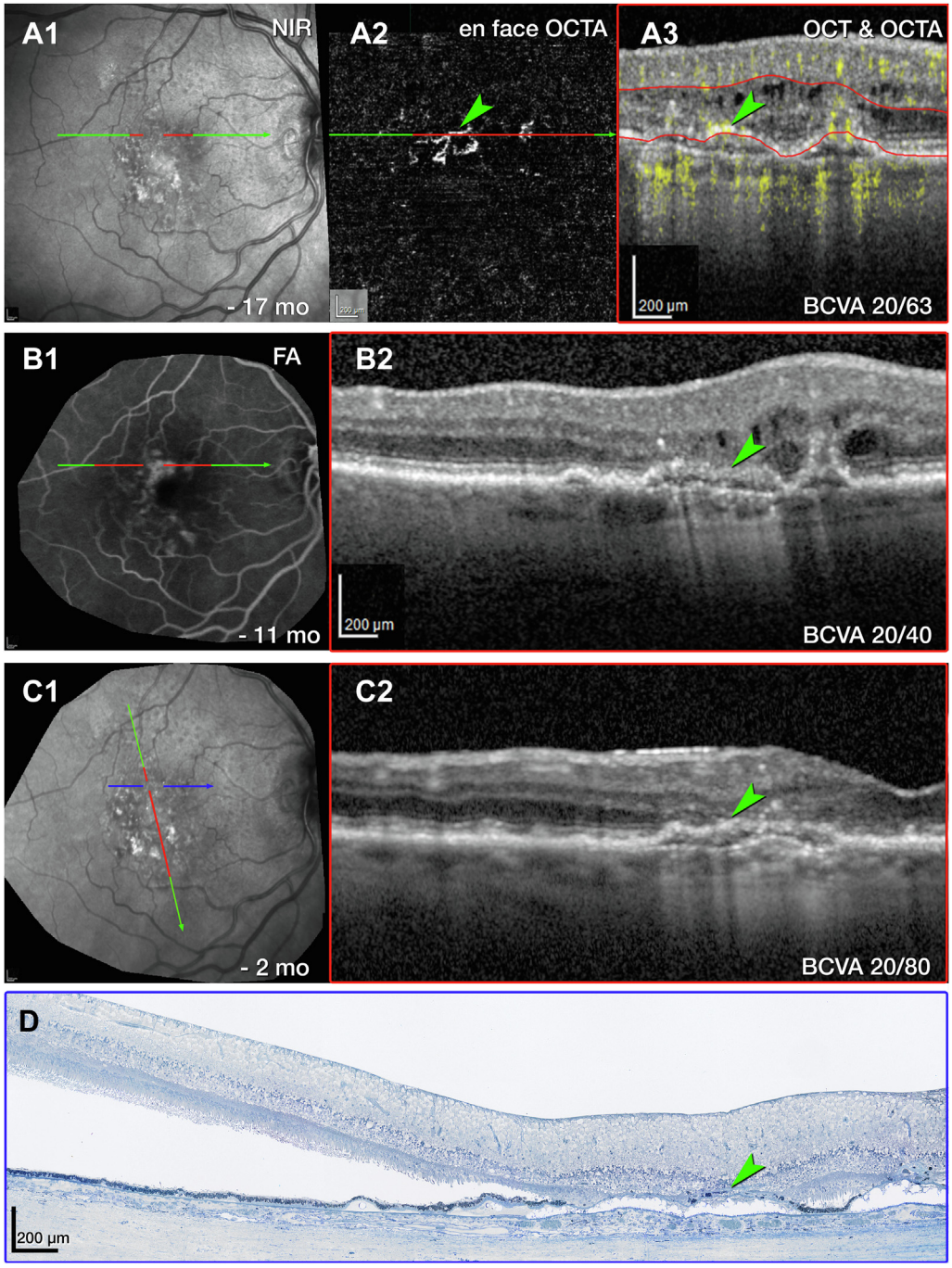

Figure 8. Multimodal imaging, clinical course, and histology of tangled type 3 macular neovascularization (MNV), right eye (OD) 1. **A**, Green and red lines on near-infrared reflectance imaging (NIR) (**A1**) represent OCT B-scans corresponding to en face OCT angiography (OCTA) (**A2**) and OCT B-scan with flow signal overlay (**A3**). After 29 total injections and 8 weeks after the prior injection (**A2**, **A3**), the flow signal persists within the tangled hyperreflective type 3 MNV lesion (green arrowhead). The retinal pigment epithelium (RPE)/Bruch's membrane (BrM) complex is split by hyporeflective material and appears as a "double layer" sign without flow signal (**A3**). Red lines in **A2** indicate the segmentation boundaries (outer plexiform layer [OPL]—RPE) used to create the en face OCTA (**A2**). **B**, Fluorescein angiography (FA) (**B1**) shows late venous phase hyperfluorescence after 32 total injections and 8 weeks after the last injection. OCT B-scan (**B2**) shows intraretinal fluid in the inner nuclear and Henle fiber layers (HFLs) surrounding the type 3 MNV lesion (green arrowhead). **C**, NIR (**C1**) and radially oriented OCT B-scan (**C2**) show intraretinal fluid adjacent to the tangled type 3 MNV lesion (green arrowhead) after 36 total injections and 8 weeks after the prior injection. The blue line in **C1** represents the histology section in **D**. **D**, Panoramic histology shows a horizontally oriented tangled type 3 MNV lesion (green arrowhead), partly bounded by RPE cells (scale bar = 200 µm). The complex extends from the inner nuclear layer (INL) border to a chipped-out calcified druse, which correlates to the double layer sign in **B1**. The druse is draped by a basal laminar deposit (BLamD) and lacks RPE at its apex. Time in months, time before death. BCVA = best corrected visual acuity.

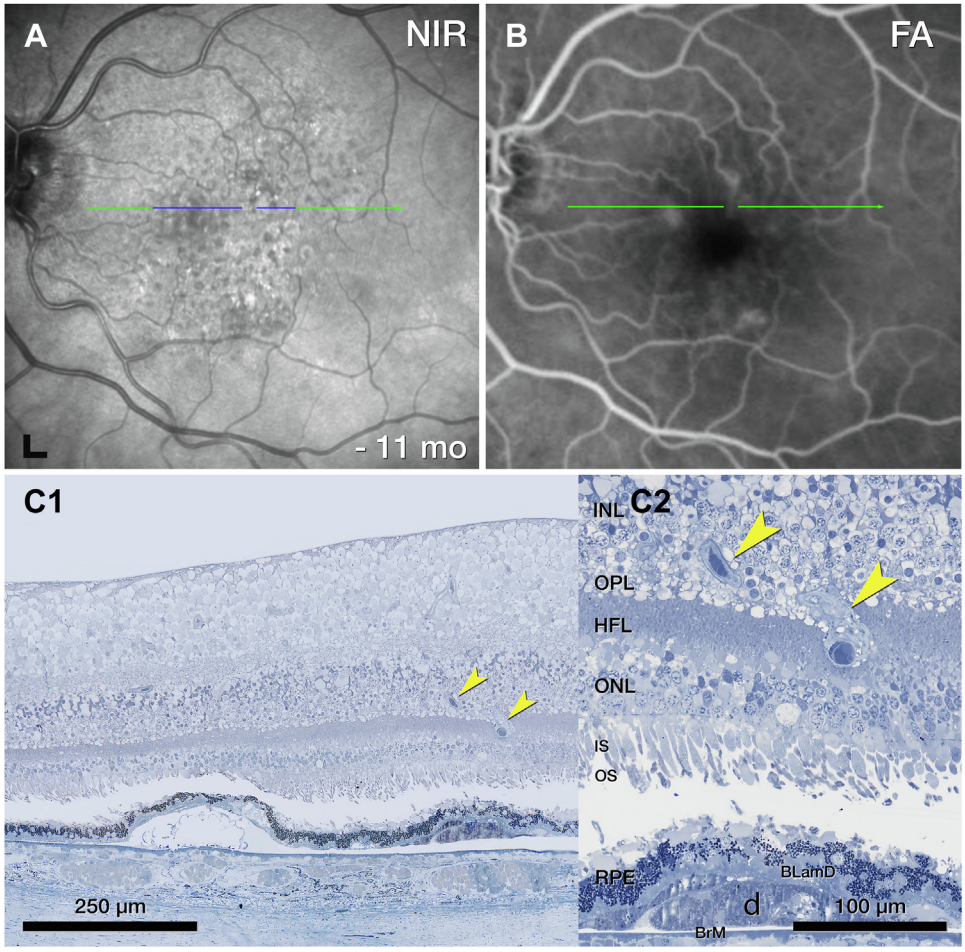

Figure 11. Deep retinal age-related microvascular anomaly (DRAMA), OS1. **A**, Near-infrared reflectance (NIR) shows drusen and subretinal drusenoid deposits 11 months before death. Blue line, plane of histology section. **B**, The fluorescein angiography (FA) recirculation phase shows minimal leakage at the site of DRAMA. **C**, On histology, a vessel extends downward (yellow arrowheads) from the inner nuclear layer (INL) into the outer plexiform layer (OPL) above a druse. BLamD = basal laminar deposit; HFL = Henle fiber layer; IS = inner segment; ONL = outer nuclear layer; RPE = retinal pigment epithelium.

OS 1 includes a vessel extending from the INL into the ONL (Fig 11A). Like type 3 MNV lesions, this DRAMA lesion is located above a soft druse with BLamD and altered RPE at its apex (Fig 11C). Unlike type 3 MNV, OS 1 does not have a collagenous sheath, and the OPL does not subside (Fig 11C2).

Corresponding to FA, OCT of OS 3 shows an intraretinal hyperreflective, stacked lesion without intraretinal cysts (Fig 12A). Over time, a plume of HRF extends nasally, still without evidence of cysts (Fig 12C).[42,43] In histology, an RPE tower atop a soft druse extends into the OPL (Fig 12D). This RPE complex surrounds like a gripping hand a vessel extending downward from the DCP (Fig 13A, B). By light microscopy, the extending vessel in OS 3 resembles DRAMA OS 1 (Fig 11) in its location above a soft druse with thick BLamD and a thinned RPE layer. By transmission electron microscopy, OS 3 (Fig S14, available at www.ophthalmologyscience.org) resembles type 3 MNV lesions but lacks a collagenous sheath. Endothelial cells in OS 3 lack fenestrations (Fig 13C) like endothelial cells of the DCP and unlike endothelial cells of the choriocapillaris (Fig 13D, E) Other vessel wall components cannot be identified. The RPE complex is multicellular with some multinucleated cells (Fig S14). Organelle packing and electron density are similar to in-layer RPE cells (not shown).

OCT angiography flow overlay of DRAMA OD 3 shows an intraretinal hyperreflective lesion containing a pair of vascular outpouchings (Fig 15C, D). Corresponding histology displays a pair of deeply descending vessels without significant intraretinal fluid (Fig 15E). Similar to type 3 MNV, the vessel complex of this DRAMA is ensheathed by a thin layer of collagenous material and dives from the INL into the HFL (Fig 16A). Unlike type 3 MNV, the vessels do not extend past the HFL, and there is no subsidence of the ELM. Retinal pigment epithelium organelles appear near the vessel complex (Fig 16B).

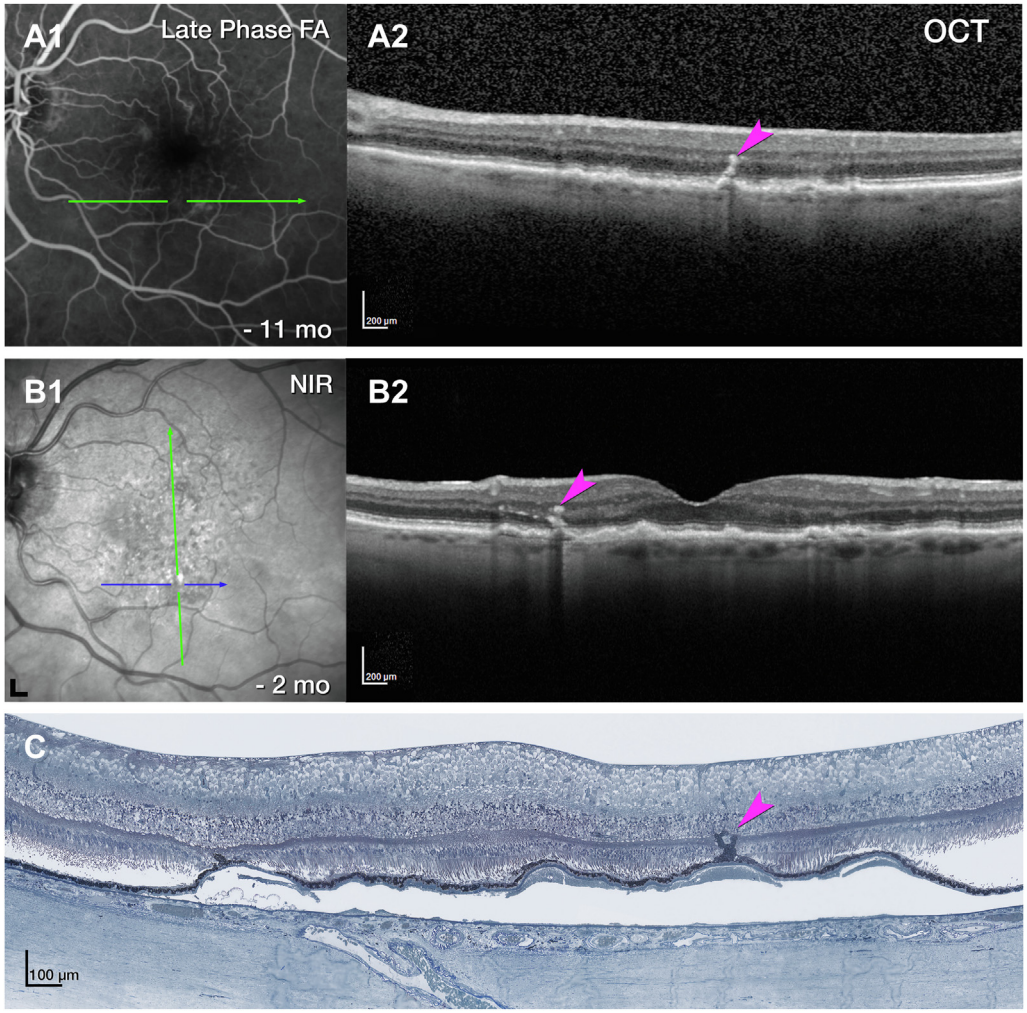

Figure 12. Multimodal imaging and histology of deep retinal age-related microvascular anomaly (DRAMA) with intraretinal retinal pigment epithelium (RPE) complex, left eye (OS) 3. **A**, Fluorescein angiography (FA) venous phase shows faint staining, 11 months before death (**A1**). OCT (**A2**) shows a stack of intraretinal hyperreflective foci (HRF) (fuchsia arrowhead). No intraretinal cysts were visible. **B**, After 6 total injections and 6 weeks after the prior injection, the stacked lesion (fuchsia arrowhead) was stable without cysts. A plume of HRF extended nasally 2 months before death. Green lines, OCT B-scans; blue line, histology section. **C**, On histology, an RPE tower (fuchsia arrowhead) rises upward from a soft druse. Cells surround a vessel and extend into the outer plexiform layer (OPL). Magnified histology is shown in Figure 9. NIR = near-infrared reflectance.

Vessel Diameters of Vascular Lesions and Comparison Vessels

Table S3 (available at www.ophthalmologyscience.org) shows internal and external vessel diameters of type 3 MNV and DRAMA, as well as DCP vessels in the index case and donor eyes (8 intermediate AMD, 83.4 ± 11.6 years; 8 controls, 84.1 ± 6.7 years). Five of the 6 index case lesions are noticeably larger (2.5- to 3-fold) than the comparison vessels. External vessel diameters of type 3 MNV (OD 1, 15.02 ± 3.81 µm; OD 2, 21.35 ± 10.79 µm; and OS 4 12.46 ± 0.95 µm) are larger than nearby DCP diameters (7.18 ± 1.11 µm). They are also larger than vessel diameters in intermediate AMD (6.79 ± 1.05 µm) and control (7.86 ± 1.47 µm, Table S3A) eyes. In DRAMA, the external vessel diameters of OS 1 and OS 3 (13.39 ± 2.68 µm; 17.97 ± 1.08 µm) are considerably larger than the comparison vessels. A similar pattern is seen for internal vessel diameters (Table S3B).

An overview of the unifying and distinguishing features of type 3 MNV and DRAMA, combining this and prior reports, is provided in Table 4.[3,16,24]

Discussion

In 2 anti-VEGF–treated eyes of 1 patient with neovascular AMD, we compare longitudinal multimodal clinical imaging and histology of type 3 MNV and DRAMA (Tables 2 and 4). This one patient had clinical and imaging characteristics typical of multifocal type 3 MNV, including bilateral presentation[44] and absence of type 1 MNV.[11–13,44,45] Type

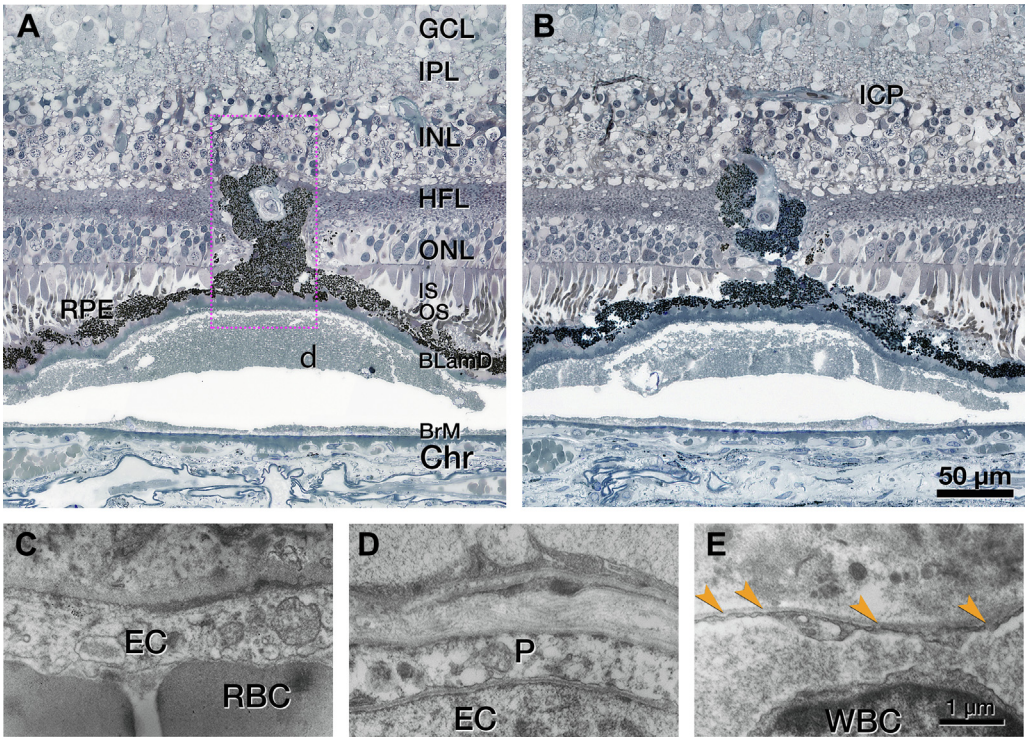

Figure 13. Retinal pigment epithelium (RPE) complex associated with deep retinal age-related microvascular anomaly (DRAMA), left eye (OS) 3. **A**, A "hand"-shaped complex consisting of RPE cells surrounds the vessel extending downward from the deep capillary plexus (DCP). Electron microscopy of the area in the dotted fuchsia box is shown in Figure S14. **B**, The RPE complex extends upward to the inner nuclear layer (INL). On either side of this complex, there is no subsidence of the outer plexiform layer (OPL) or external limiting membrane (ELM), and the outer nuclear layer (ONL) is thinned. The complex emanates from a continuous RPE layer over the basal laminar deposit (BLamD) and a soft druse. The druse is artifactually detached from Bruch's membrane (BrM). **C**–**E**, Endothelial cell (EC) ultrastructure in DRAMA and comparison vessels are shown. The vascular lumen is at the bottom of all panels. **C**, No fenestrations are visible in the DRAMA (red blood cell [RBC]). **D**, No fenestrations were visible in the DCP (pericyte [P]). **E**, Fenestrations are visible in the choriocapillaris endothelium (orange arrowheads; white blood cell [WBC]). Ch = choroid; GCL = ganglion cell layer; HFL = Henle fiber layer; ICP = intermediate capillary plexus; IPL = inner plexiform layer; IS = inner segment.

3 MNV is distinguished by intraretinal origin,[1,2,46] frequent near-term bilateral involvement,[7–9] and significant choroidal thinning with reduced perfusion.[47,48]

Patients with type 3 MNV are older at initial diagnosis than patients with type 1 MNV.[49,50]

In our case, treated type 3 MNV has 2 morphologic phenotypes: pyramidal (OD 2 and OS 4) or tangled (OD 1). All 3 analyzed complexes originate at the DCP and extend posteriorly to approach persistent BLamD but do not enter the sub–RPE-BL space or cross BrM. These 2 phenotypes may correspond to those seen by Borelli et al[14] in treatment-naive type 3 MNV eyes with rotational 3-dimensional OCTA. These authors describe 26 lesions as "filiforms" and 9 lesions as "saccular," which seem similar in shape to pyramidal (filiform) and tangled (saccular).[14] We also find more pyramidal lesions than tangled. It remains to be determined if saccular and filiform lesions differ in spatial distribution and time of onset.[14]

Our previous description of pyramidal type 3 MNV included endothelial cells in a thick collagenous matrix and dysmorphic RPE cells scattered along the neovascular stalk.[16] OD 2 and OS 4 in this case[3] add pericytes plus a nearly continuous covering by highly pigmented RPE (OS 4), supporting the early involvement of migratory RPE.[2,51] The sheath distinguishes lesions from unaffected DCP vessels. The main differences between pyramidal and tangled lesions are the larger horizontal extent and thinner collagenous sheath of tangled.[3] Endothelial cells of tangled vessels, and presumably also those in the pyramidal, lack fenestrations like the source vessels in the DCP.

As before,[16] we did not see vessels of choroidal origin in the sub–RPE-BL space, as reported for advanced type 3 MNV.[14,44,52–54] Nor did we see DCP-originating vessels penetrate through the BLamD and enter the sub–RPE-BL space. This depth of penetration was suggested as necessary for exudation.[55] This proposal was based on OCTA imaging without projection artifact removal to reduce spurious signal directly under type 3 MNV.[55] Using volumetric artifact removal, we did not see an OCTA flow signal in the sub–RPE-BL space (Fig 8A3). It is possible that anti-VEGF treatment rendered invisible downward projections from the DCP or upward projections from the choriocapillaris. We think this is unlikely because neocapillaries may shrink after treatment, but they do not disappear.[56,57] Furthermore, our use of stepped sections may miss key

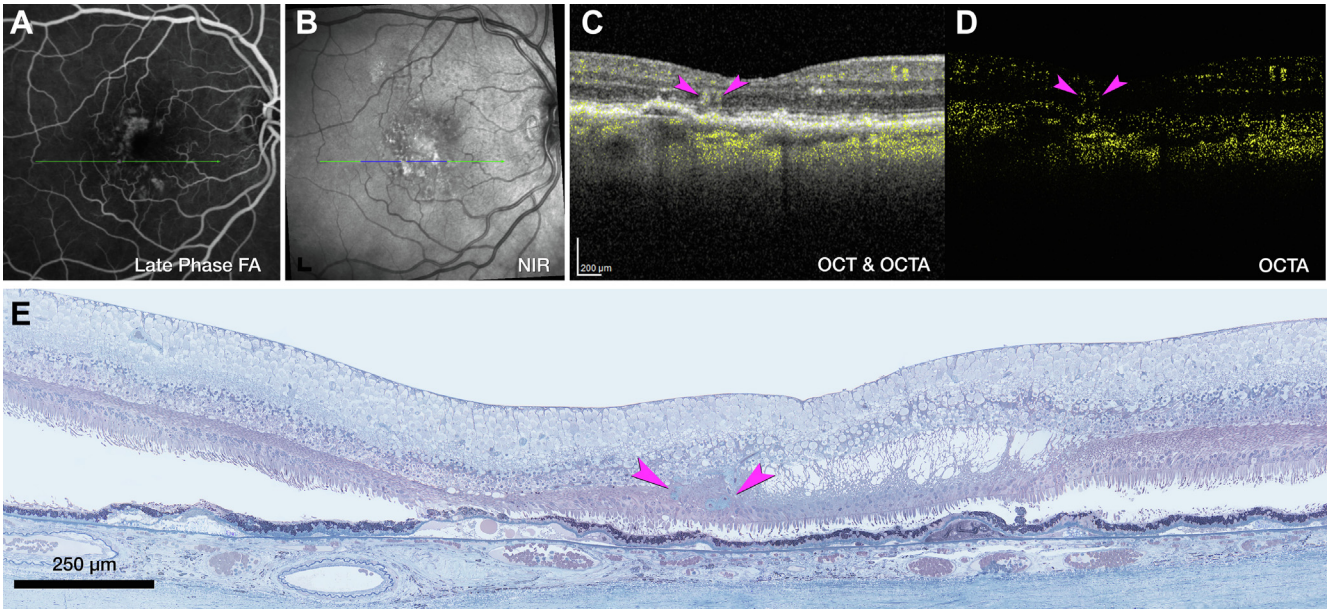

Figure 15. Multimodal imaging of deep retinal age-related microvascular anomalies (DRAMAs) right eye (OD) 3. **A**, Fluorescein angiography (FA) venous phase showed mild hyperfluorescence 11 months before death. **B**, Green and blue lines on near-infrared reflectance (NIR) represent OCT B-scan (**C**) and histology section (**D**). **C**, Horizontally oriented OCT B-scan with OCT angiography (OCTA) flow overlay shows cystlike spaces in the Henle fiber layer (HFL) adjacent to a pair of hyperreflective DRAMAs (fuchsia arrowheads). The retinal pigment epithelium (RPE)/Bruch's membrane (BrM) complex to the left is split by hyporeflective material. **D**, OCTA shows a pair of intraretinal flow signals (fuchsia arrowheads). **E**, Histology shows a pair of vessels extending from the inner nuclear layer (INL) border to the outer nuclear layer (ONL). Magnified histology is shown in Figure 11.

details. Nevertheless, in all analyzed sections of this case, both BLamD and BrM were intact. Longitudinal imaging before exudation onset is needed to understand this phase of type 3 MNV progression.

The thick collagenous sheath of type 3 MNV lesions may impact clinical monitoring as follows. All lesions responded to anti-VEGF with temporary resolution of exudation and persistence over several fluid absorption cycles.

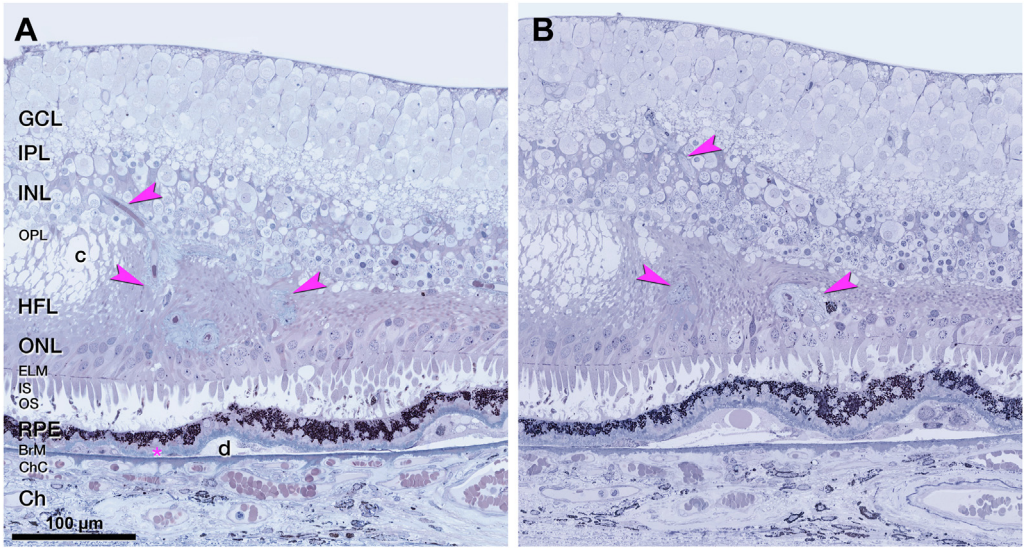

Figure 16. Vascular complex of deep retinal age-related microvascular anomaly (DRAMA), OD 3. **A**, **B**, A penetrating pair of vessels (DRAMAs, fuchsia arrowheads), ensheathed by collagenous material, dives from the inner nuclear layer (INL) into the Henle fiber layer (HFL)/outer nuclear layer (ONL). Next to the vessels is a degenerative cyst in the HFL. There is no subsidence of the external limiting membrane (ELM). The ONL was thinned. **B**, Retinal pigment epithelium (RPE) from the edge of a druse (d) migrates toward the lower edge of the vessel complex, right side. BrM = Bruch's membrane; Ch = choroid; ChC = choriocapillaris; GCL = ganglion cell layer; IPL = inner plexiform layer; IS = inner segment; OS = left eye; OPL = outer plexiform layer.

Table 4. Features of Type 3 MNV and DRAMA Compared

Feature	Type 3 MNV Pyramidal	Type 3 MNV-Tangled	DRAMA
Location, topographic	ETDRS inner	ETDRS inner	ETDRS inner
Location, layer	HFL/ONL	HFL/ONL	HFL/ONL
RPE	Absent, scattered, migrated	Absent, scattered, migrated	Migrated, intact
ELM	Descent	Descent	Horizontal
Sub–RPE-BL space	End stages of soft drusen*	End stages of soft drusen*	Soft drusen, cells
Originating plexus	DCP	DCP	DCP
Shape of the vascular complex	Compact, base-down pyramid	Vertical, horizontally spreading	Downward extending loop
Structure over time	Dynamic	Dynamic	Stable[24]
Pericytes	Yes	Yes	Yes
Exudation	Yes	Yes	No
Anti-VEGF response	Yes	Yes	No
Collagenous sheath	Thick	Thin	None/thin if advanced
Endothelium	Nonfenestrated	Nonfenestrated	Nonfenestrated

Based on the current and published data.[3,16,24]
BL = basal lamina; DCP = deep capillary plexus; DRAMA = deep retinal age-related microvascular anomaly; ELM = external limiting membrane; HFL = Henle fiber layer; MNV = macular neovascularization; ONL = outer nuclear layer; RPE = retinal pigment epithelium.
*Calcific nodules, cells (subducted RPE, macrophages, giant cells, fibroblasts), Müller glia, and avascular fibrosis.

By OCTA, some early-stage lesions regress completely, whereas treatment of later-stage lesions requires continuing therapy.[2,54] Furthermore, treated type 3 MNV lesions can reappear after becoming undetectable on OCTA.[55,58] Lesions with thick sheaths remain detectable by structural OCT long after treatment.[57] The collagenous neovascular stalk was populated by endothelial cells and pericytes that either remained, self-renewed, or migrated in during VEGF cycles. We can speculate that the sheath structurally stabilizes endothelial cells within it and that both VEGF and anti-VEGF agents impact lesions principally where the sheath is absent. If MNV persistence after treatment, as well as recurrence after apparent regression, is influenced by sheaths, then monitoring for disease activity by vascular characteristics in addition to fluid may be useful.

We showed that type 3 MNV can coexist with vascular formations that are candidate precursors, early stages, and masqueraders for type 3 MNV. All 3 DRAMAs originated from the DCP and extended posteriorly into the HFL. None of the DRAMA lesions involved the superficial capillary plexus, and no significant intraretinal fluid was detectable on OCT over time. Like type 3 MNV (Fig S10), 1 DRAMA had nonfenestrated endothelial cells and pericytes (Fig S14). Unlike type 3 MNV and like native DCP, 2 DRAMAs lacked a collagenous sheath. The 1 DRAMA with a thin sheath (OD 3) also extended the furthest of the 3 into the ONL, perhaps indicating chronicity. Importantly, none of the DRAMAs were accompanied by the descent of the ELM, the border of atrophy in the neurosensory retina, although the ELM can be perforated by inwardly migrating RPE, as in OS 3. It is unlikely that DRAMAs in our case represent exudative perifoveal vascular anomalous complexes or nonexudative perifoveal vascular anomalous complexes,[31,35,36] which typically appear above the DCP. Microvascular anomalies in eyes with neovascular and nonneovascular AMD include capillary dilations and telangiectasia that are associated with locally increased VEGF expression.[17,59–61] A recent study showed that 19 of 94 eyes with type 3 MNV exhibited an asymptomatic precursor stage on OCT.[44] Because lack of exudation and nonprogression to type 3 MNV in our case might result from VEGF suppression,[62] longitudinal imaging is required to definitively place DRAMA in the progression sequence of type 3 MNV.

All analyzed vessels localized within 500 to 1500 μm of the foveal center, aligned with similar findings for solitary and multifocal lesions.[11,12] A role for choroidal ischemia is hypothesized[11,63–65] because the choroid is thinner in eyes with type 3 MNV than in eyes with types 1 and 2 MNV.[66,67] The radial symmetry of lesions around and close to the fovea further suggests an association with the distribution of photoreceptors and their support cells, which vary markedly in this eccentricity range. The ETDRS inner ring of type 3 MNV vulnerability is just peripheral to the foveal avascular zone[33] on the inner slope of the crest of high rod density. Rod vision in AMD eyes is poorest in the same area.[68–72] Metabolic demand of foveal cones is high, and the choriocapillaris OCTA signal decreases under the fovea throughout adulthood.[73,74] It is thus possible that the distribution of type 3 MNV is an additional effect of microvascular changes under the fovea that also contribute to high-risk drusen and reduced sustenance of nearby rods.

Study strengths include the availability of OCTA with eye-tracked OCT, volumetric projection artifact removal, rapid tissue preservation to largely maintain retinal attachment, registration of premortem and postmortem OCT volumes, and comprehensive histologic and microscopy techniques to reveal vessels and perivascular tissue elements. Limitations include the lack of longitudinal OCTA imaging[9,75] and lack of color fundus photography to reveal discoloration patterns typical of type 3 MNV.[14] Limitations to the laboratory study included the use of stepped sections, lack of electron microscopy for all lesions, and lack of immunohistochemistry to support cell-type identifications

based on morphologic criteria. Finally, observations from 1 patient, however detailed, cannot elucidate the full range of biologic variability.

Nevertheless, our study helped define the morphologies of type 3 MNV and proposed precursors that might guide future research, diagnosis, and disease monitoring. The presence and extent of a collagenous sheath distinguishes type 3 MNV from normal DCP vessels and may represent a stage in the evolution of DRAMA toward type 3 MNV. Our hypotheses can be tested in the larger samples available in clinic populations and clinical trial imaging datasets, ideally before the onset of exudation.

Footnotes and Disclosures

Originally received: September 19, 2022.
Final revision: January 16, 2023.
Accepted: January 30, 2023.
Available online: February 10, 2023.Manuscript no. XOPS-D-22-00199R2.

[1] Department of Ophthalmology and Visual Sciences, Heersink School of Medicine, University of Alabama at Birmingham, Birmingham, Alabama.

[2] Department of Ophthalmology, University Hospital Wurzburg, Wurzburg, Germany.

[3] Vitreous Retina Macula Consultants of New York, New York.

[4] NOVA Medical School Research, Universidade NOVA de Lisboa, Lisbon, Portugal.

[5] The First Affiliated Hospital of Chongqing Medical University, Chongqing Key Laboratory of Ophthalmology, and Chongqing Eye Institute, Chongqing, China.

[6] Centre for Ophthalmology and Visual Science, University of Western Australia, Perth, Western Australia, Australia.

[7] Lions Eye Institute, Nedlands, Western Australia, Australia.

[8] Department of Ophthalmology, Sir Charles Gairdner Hospital, Nedlands, Western Australia, Australia.

[9] Canberra Retina Center, Canberra, Australia.

[10] Genentech, South San Francisco, California.

[11] Department of Ophthalmology, New York University Grossman School of Medicine, New York, New York.

Presented as part of an abstract to the annual meeting of the Association for Research in Vision & Ophthalmology (ARVO) May 2021 (online conference) and May 2022, Denver, Colorado.

Disclosures:

All authors have completed and submitted the ICMJE disclosures form.

The authors made the following disclosures: A.B.: Financial support − Dr Werner Jackstaedt Foundation.

K.B.F.: Consultant − Genentech, Zeiss, Heidelberg Engineering, Allergan, Bayer, Novartis.

C.A.C.: Financial support − Regeneron (outside this project).

D.F.: Employee − Genentech; Stocks − Roche.

D.C.: Financial support − Studentship from Fundação Luso-Americana para o desenvolvimento (FLAD, USA R&D@PhD − Proj 2020/0140)

The other authors have no proprietary or commercial interest in any materials discussed in this article.

Supported by Genentech/Hoffman LaRoche, The Macula Foundation, Inc., New York, NY; unrestricted funds to the Department of Ophthalmology and Visual Sciences (UAB) from Research to Prevent Blindness, Inc., and the EyeSight Foundation of Alabama. The purchase of the slide scanner was made possible by the Carl G. and Pauline Buck Trust.

The sponsors had no role in the design and conduct of the study; collection, management, analysis, and interpretation of the data; preparation, review, or approval of the manuscript, and decision to submit the manuscript for publication.

HUMAN SUBJECTS: Human subjects were included in this study. The tissue donor provided informed consent. Approval for this study was obtained by an institutional review board at the University of Alabama at Birmingham (protocol #300004907). The study was conducted in accordance with the tenets of the Declaration of Helsinki and the Health Insurance Portability and Accountability Act of 1996.

No animal subjects were used in this study.

Author Contributions:

Conception and design: Berlin, Cabral, Chen, Messinger, Balaratnasingam, Mendis, Ferrara, Freund, Curcio.

Data collection: Berlin, Cabral, Chen, Messinger, Balaratnasingam, Mendis, Ferrara, Freund, Curcio.

Analysis and interpretation: Berlin, Cabral, Chen, Messinger, Balaratnasingam, Mendis, Ferrara, Freund, Curcio.

Obtained funding: Curcio, Berlin, Freund, Ferrara

Overall responsibility: Berlin, Cabral, Chen, Messinger, Balaratnasingam, Mendis, Ferrara, Freund, Curcio.

Abbreviations and Acronyms:
AMD = age-related macular degeneration; **BL** = basal lamina; **BLamD** = basal laminar deposit; **BrM** = Bruch membrane; **DCP** = deep capillary plexus; **DRAMA** = deep retinal age-related microvascular anomalies; **ELM** = external limiting membrane; **FA** = fluorescein angiography; **HFL** = Henle fiber layer; **HRF** = hyperreflective foci; **INL** = inner nuclear layer; **MNV** = macular neovascularization; **OCTA** = OCT angiography; **OD** = right eye; **ONL** = outer nuclear layer; **OPL** = outer plexiform layer; **OS** = left eye; **RPE** = retinal pigment epithelium.

Keywords:
Age-related macular degeneration, Deep retinal age-related microvascular anomalies, Histopathology, Type 3 macular neovascularization, Vascular morphology.

Correspondence:
Christine A. Curcio, PhD, 1670 University Boulevard Room 360, Birmingham, AL 35294-0019. E-mail: christinecurcio@uabmc.edu.

References

1. Freund KB, Zweifel SA, Engelbert M. Do we need a new classification for choroidal neovascularization in age-related macular degeneration? *Retina*. 2010;30:1333−1349.

2. Su D, Lin S, Phasukkijwatana N, et al. An updated staging system of type 3 neovascularization using spectral domain optical coherence tomography. *Retina*. 2016;36:S40−S49.

3. Berlin A, Cabral D, Chen L, et al. Correlation of optical coherence tomography angiography of type 3 macular neovascularization with corresponding histology. *JAMA Ophthalmol*. 2022;140:628−633.
4. Spaide RF, Jaffe GJ, Sarraf D, et al. Consensus nomenclature for reporting neovascular age-related macular degeneration data: consensus on neovascular age-related macular degeneration nomenclature study group. *Ophthalmology*. 2020;127:616−636.
5. Yannuzzi LA, Negrão S, Iida T, et al. Retinal angiomatous proliferation in age−related macular degeneration. *Retina*. 2012;32:416−434.
6. Jung JJ, Chen CY, Mrejen S, et al. The incidence of neovascular subtypes in newly diagnosed neovascular age-related macular degeneration. *Am J Ophthalmol*. 2014;158:769−779.e2.
7. Kim JH, Kim JW, Kim CG, Lee DW. Influence of fellow-eye examination interval on visual acuity at fellow-eye neovascularization in unilateral type 3 neovascularization. *Retina*. 2020;40:1255−1261.
8. Kwak JH, Park WK, Kim RY, et al. Unaffected fellow eye neovascularization in patients with type 3 neovascularization: incidence and risk factors. *PloS One*. 2021;16:e0254186.
9. Sacconi R, Forte P, Capuano V, et al. optical coherence tomography angiographycharacterization of evolving lesions in fellow eyes of exudative type 3 macular neovascularization patients. *Retina*. 2022;42:2075−2082.
10. Freund KB, Ho IV, Barbazetto IA, et al. Type 3 neovascularization: the expanded spectrum of retinal angiomatous proliferation. *Retina*. 2008;28:201−211.
11. Najeeb BH, Deak G, Schmidt-Erfurth U, Gerendas BS. The RAP study report two: the regional distribution of macular neovascularization type 3, a novel insight into its etiology. *Retina*. 2020;40:2255−2262.
12. Haj Najeeb B, Deak GG, Sacu S, et al. The RAP study, report 4: morphological and topographical characteristics of multifocal macular neovascularization type 3. *Graefes Arch Clin Exp Ophthalmol*. 2022;260:141−147.
13. Haj Najeeb B, Deak GG, Schmidt-Erfurth U, Gerendas BS. The RAP study, report 3: discoloration of the macular region in patients with macular neovascularization type 3. *Acta Ophthalmol*. 2022;100:e270−e277.
14. Borrelli E, Sacconi R, Klose G, et al. Rotational three-dimensional OCTA: a notable new imaging tool to characterize type 3 macular neovascularization. *Sci Rep*. 2019;9:17053.
15. Shimada H, Kawamura A, Mori R, Yuzawa M. Clinicopathological findings of retinal angiomatous proliferation. *Graefes Arch Clin Exp Ophthalmol*. 2007;245:295−300.
16. Li M, Dolz-Marco R, Messinger JD, et al. Clinicopathologic correlation of anti-vascular endothelial growth factor−treated type 3 neovascularization in age-related macular degeneration. *Ophthalmology*. 2018;125:276−287.
17. Sacconi R, Freund KB, Yannuzzi LA, et al. The expanded spectrum of perifoveal exudative vascular anomalous complex. *Am J Ophthalmol*. 2017;184:137−146.
18. Gilani F, Gal-Or O, Freund KB. Spontaneous rupture and involution of a "macro−microaneurysm" in diabetic retinopathy. *Retina*. 2017;37:e73e4.
19. Spaide RF, Barquet LA. Retinal capillary macroaneurysms. *Retina*. 2019;39:1889−1895.
20. Sacconi R, Cohen SY, Borrelli E, et al. *Correspondence.* Retina. 2019;39:e48−e49.
21. Spaide RF. *Reply.* Retina. 2019;39:e49−e50.
22. Sacconi R, Borrelli E, Sadda S, et al. Nonexudative perifoveal vascular anomalous complex: the subclinical stage of perifoveal exudative vascular anomalous complex? *Am J Ophthalmol*. 2020;218:59−67.
23. Querques G, Kuhn D, Massamba N, et al. Perifoveal exudative vascular anomalous complex. *J Fr Ophtalmol*. 2011;34:559.e1−e4.
24. Cabral D, Ramtohul P, Fradinho AC, Freund KB. Volume rendering of deep retinal age-related microvascular anomalies. *Ophthalmol Retina*. 2022;6:1185−1193.
25. Chen L, Messinger JD, Sloan KR, et al. Nonexudative macular neovascularization supporting outer retina in age-related macular degeneration: a clinicopathologic correlation. *Ophthalmology*. 2020;127:931−947.
26. Querques G, Querques L, Forte R, et al. Precursors of type 3 neovascularization: a multimodal imaging analysis. *Retina*. 2013;33:1241−1248.
27. World Medical Association. World Medical Association Declaration of Helsinki: ethical principles for medical research involving human subjects. *JAMA*. 2013;310:2191−2194.
28. Edemekong P, Annamaraju P, Haydel M. *Health Insurance Portability and Accountability Act. StatPearls Treasure Island (FL)*. StatPearls Publishing; 2021.
29. Rocholz R, Teussink M, Dolz-Marco R, et al. SPECTRALIS optical coherence tomography angiography (OCTA): principles and clinical applications. *Heidelb Eng Acad*. 2018;1−10.
30. Cabral D, Fradinho AC, Pereira T, et al. Macular vascular imaging and connectivity analysis using high-resolution optical coherence tomography. *Transl Vis Sci Technol*. 2022;11:2.
31. Breazzano MP, Bacci T, Curcio CA, Freund KB. Novel multimodal imaging and volume rendering of type 3 macular neovascularization. *Retina*. 2020;40:e55−e57.
32. Xu X, Yannuzzi NA, Fernández-Avellaneda P, et al. Differentiating veins from arteries on optical coherence tomography angiography by identifying deep capillary plexus vortices. *Am J Ophthalmol*. 2019;207:363−372.
33. Kim JH, Chang YS, Kim JW, et al. Characteristics of type 3 neovascularization lesions: focus on the incidence of multifocal lesions and the distribution of lesion location. *Retina*. 2020;40:1124−1131.
34. Early Treatment of Diabetic Retinopathy Study Group. Grading diabetic retinopathy from stereoscopic color fundus photographs—an extension of the modified Airlie House classification: ETDRS report number 10. *Ophthalmology*. 1991;98:786−806.
35. Pongsachareonnont P, Somkijrungroj T, Assavapongpaiboon B, et al. Foveal and parafoveal choroidal thickness pattern measuring by swept source optical coherence tomography. *Eye (Lond)*. 2019;33:1443−1451.
36. Balaratnasingam C, An D, Sakurada Y, et al. Comparisons between histology and optical coherence tomography angiography of the periarterial capillary-free zone. *Am J Ophthalmol*. 2018;189:55−64.
37. Litts KM, Messinger JD, Dellatorre K, et al. Clinicopathological correlation of outer retinal tubulation in age-related macular degeneration. *JAMA Ophthalmol*. 2015;133:609−612.
38. Balaratnasingam C, An D, Freund KB, et al. Correlation between histologic and OCT angiography analysis of macular circulation. *Ophthalmology*. 2019;126:1588−1589.
39. Berlin A, Ferrara D, Freund KB, Curcio CA. OCT features relevant to neovascular AMD management and non-neovascular AMD progression: clinicopathologic correlation.

Retinal Cases Brief Rep. 2022. https://doi.org/10.1097/ICB.0000000000001356.
40. Berlin A, Chen L, Messinger J, et al. Double-layer sign in neovascular age-related macular degeneration—do we treat? *Acta Ophthalmol*. 2022;100:348—349.
41. Snodderly DM, Weinhaus RS, Choi JC. Neural-vascular relationships in central retina of macaque monkeys (Macaca fascicularis). *J Neurosci*. 1992;12:1169—1193.
42. Balaratnasingam C, Messinger JD, Sloan KR, et al. Histologic and optical coherence tomographic correlates in drusenoid pigment epithelium detachment in age-related macular degeneration. *Ophthalmology*. 2017;124:644—656.
43. Cao D, Leong B, Messinger JD, et al. Hyperreflective foci and optical coherence tomography progression indicators in age-related macular degeneration include transdifferentiated retinal pigment epithelium. *Invest Ophthalmol Vis Sci*. 2021;62:34.
44. Najeeb BH, Deak GG, Mylonas G, et al. The RAP study, report 5: rediscovering macular neovascularization type 3: multimodal imaging of fellow eyes over 24 months. *Retina*. 2022;42:485—493.
45. Najeeb BH, Deak GG, Schmidt-Erfurth UM, Gerendas BS. RAP study, report 1: novel subtype of macular neovascularisation type III, cilioretinal MNV3. *Br J Ophthalmol*. 2021;105:113—117.
46. Querques G, Souied EH, Freund KB. How has high-resolution multimodal imaging refined our understanding of the vasogenic process in type 3 neovascularization? *Retina*. 2015;35:603—613.
47. Borrelli E, Souied EH, Freund KB, et al. Reduced choriocapillaris flow in eyes with type 3 neovascularization and age-related macular degeneration. *Retina*. 2018;38:1968—1976.
48. Koizumi H, Iida T, Saito M, et al. Choroidal circulatory disturbances associated with retinal angiomatous proliferation on indocyanine green angiography. *Graefes Arch Clin Exp Ophthalmol*. 2008;246:515—520.
49. Caramoy A, Ristau T, Lechanteur YT, et al. Environmental and genetic risk factors for retinal angiomatous proliferation. *Acta Ophthalmol*. 2014;92:745—748.
50. Daniel E, Shaffer J, Ying GS, et al. Outcomes in eyes with retinal angiomatous proliferation in the comparison of age-related macular degeneration treatments trials (CATT). *Ophthalmology*. 2016;123:609—616.
51. Spaide RF. Fundus autofluorescence and age-related macular degeneration. *Ophthalmology*. 2003;110:392—399.
52. Yannuzzi LA, Freund KB, Takahashi BS. Review of retinal angiomatous proliferation or type 3 neovascularization. *Retina*. 2008;28:375—384.
53. Cho HJ, Lim SH, Kim J, et al. Assessing the long-term evolution of type 3 neovascularization in age-related macular degeneration using optical coherence tomography angiography. *Graefes Arch Clin Exp Ophthalmol*. 2021;259:2605—2613.
54. Kim JH, Chang YS, Kim JW, et al. Difference in treatment outcomes according to optical coherence tomography-based stages in type 3 neovascularization (retinal angiomatous proliferation). *Retina*. 2018;38:2356—2362.
55. Sacconi R, Battista M, Borrelli E, et al. OCT-A characterisation of recurrent type 3 macular neovascularisation. *Br J Ophthalmol*. 2021;105:222—226.
56. Huang D, Jia Y, Rispoli M, et al. OCT angiography of time course of choroidal neovascularization in response to anti-angiogenic treatment. *Retina*. 2015;35:2260—2264.
57. Skalet AH, Miller AK, Klein ML, et al. Clinicopathologic correlation of retinal angiomatous proliferation treated with ranibizumab. *Retina*. 2017;37:1620—1624.
58. Han JW, Cho HJ, Kang DH, et al. Changes in optical coherence tomography angiography and disease activity in type 3 neovascularization after anti—vascular endothelial growth factor treatment. *Retina*. 2020;40:1245—1254.
59. Tolentino MJ, Miller JW, Gragoudas ES, et al. Intravitreous injections of vascular endothelial growth factor produce retinal ischemia and microangiopathy in an adult primate. *Ophthalmology*. 1996;103:1820—1828.
60. Tolentino MJ, Mcleod DS, Taomoto M, et al. Pathologic features of vascular endothelial growth factor-induced retinopathy in the nonhuman primate. *Am J Ophthalmol*. 2002;133:373—385.
61. Jackson TL, Danis RP, Goldbaum M, et al. Retinal vascular abnormalities in neovascular age-related macular degeneration. *Retina*. 2014;34:568—575.
62. Spaide RF. New proposal for the pathophysiology of type 3 neovascularization as based on multimodal imaging findings. *Retina*. 2019;39:1451—1464.
63. Hayreh SS. Segmental nature of the choroidal vasculature. *Br J Ophthalmol*. 1975;59:631—648.
64. Hayreh SS. In vivo choroidal circulation and its watershed zones. *Eye (Lond)*. 1990;4:273—289.
65. Hayreh SS. Posterior ciliary artery circulation in health and disease the Weisenfeld lecture. *Invest Ophthalmol Vis Sci*. 2004;45:749—757.
66. Yamazaki T, Koizumi H, Yamagishi T, Kinoshita S. Subfoveal choroidal thickness in retinal angiomatous proliferation. *Retina*. 2014;34:1316—1322.
67. Kim JH, Kim JR, Kang SW, et al. Thinner choroid and greater drusen extent in retinal angiomatous proliferation than in typical exudative age-related macular degeneration. *Am J Ophthalmol*. 2013;155:743—749.
68. Tan R, Guymer RH, Luu CD. Subretinal drusenoid deposits and the loss of rod function in intermediate age-related macular degeneration. *Invest Ophthalmol Vis Sci*. 2018;59:4154—4161.
69. Tan RS, Guymer RH, Aung KZ, et al. Longitudinal assessment of rod function in intermediate age-related macular degeneration with and without reticular pseudodrusen. *Invest Ophthalmol Vis Sci*. 2019;60:1511—1518.
70. Chen KG, Alvarez JA, Yazdanie M, et al. Longitudinal study of dark adaptation as a functional outcome measure for age-related macular degeneration. *Ophthalmology*. 2019;126:856—865.
71. Zhang Y, Sadda SR, Sarraf D, et al. Spatial dissociation of subretinal drusenoid deposits and impaired scotopic and mesopic sensitivity in AMD. *Invest Ophthalmol Vis Sci*. 2022;63:32.
72. Nigalye AK, Hess K, Pundlik SJ, et al. Dark adaptation and its role in age-related macular degeneration. *J Clin Med*. 2022;11:1358.
73. Zheng F, Zhang Q, Shi Y, et al. Age-dependent changes in the macular choriocapillaris of normal eyes imaged with swept-source optical coherence tomography angiography. *Am J Ophthalmol*. 2019;200:110—122.
74. Ingram NT, Fain GL, Sampath AP. Elevated energy requirement of cone photoreceptors. *Proc Natl Acad Sci USA*. 2020;117:19599—19603.
75. Borrelli E, Mastropasqua L, Souied E, et al. Longitudinal assessment of type 3 macular neovascularization using 3D volume-rendering OCTA. *Can J Ophthalmol*. 2021;57:228—235.